RSC Advances

ROYAL SOCIETY OF CHEMISTRY

www.rsc.org/advances

Synthesis and anisotropic self-assembly of Ag nanoparticles immobilized by Pluronic F127 triblock copolymer for colorimetric detection of H_2O_2†

Cong Wu [a], Guangmei Xia[b], Jing Sun[c], Rui Song *[a]

a College of Chemistry and Chemical Engineering, University of Chinese Academy of Sciences, Beijing 100049, China

b Beijing National Laboratory for Molecular Sciences, CAS Key Laboratory of Engineering Plastics, Institute of Chemistry, Chinese Academy of Sciences, Beijing 100190, China

c Shanghai Institute of Microsystem and Information Technology, Chinese Academy of Sciences, Shanghai 200050, China

Abstract

With dopamine as a reducing and sticking agent, triblock copolymers poly(ethylene oxide)-poly(propylene oxide)-poly(ethylene oxide) (PEO-PPO-PEO), Pluronic F127, was employed to immobilize and stabilize silver nanoparticles (Ag NPs) by the chemical reduction of silver nitrate, $AgNO_3$. Thus, a ternary system comprising of Ag NPs, dopamine and F127, i.e. Ag@DA@F127 system was constructed. In this ternary system, Ag NPs were anisotropically self-assembled and uniformly dispersed in the network-like F127 micelles. As evidenced that the dispersion stability of Ag NPs in this system was significantly enhanced compared to the Ag@DA and Ag@$NaHB_4$@F127 system, which in turn resulted in a more sensitive and quantitative detection of H_2O_2. Further investigation demonstrated that the Ag@DA@F127 system exhibited a UV-vis absorption band at ~405 nm and the intensity of this absorption band dramatically decreased linearly over the concentration range of 0.1~100 μM H_2O_2 (r^2 = 0.99056), deriving a detection limit of 33 nM, which was superior to recent reports. Apart from its excellent performance in H_2O_2 detection, this Ag@DA@F127 system has other benefits including facile and simple making, being environmental friendly, especially the forming of a specific

network-like structure to fully disperse Ag NPs, which makes it practical in H_2O_2 detection.

Introduction

Hydrogen peroxide (H_2O_2) is one of the most important intermediate species involved in many environmental and biological processes, and plays an important role in many fields, including industry, food, clinical laboratory, pharmaceutical and environmental analysis.[1, 2] Therefore, sensitive and reliable determination of H_2O_2 is highly demanded. In this regard, traditional methods such as chemiluminescence,[3] spectrophotometry,[4] fluorimetry[5] and electrochemistry[6] are complicated and time-consuming, while enzyme-based H_2O_2 sensors normally require harsh determination environment and expensive preparation and thus limiting its further applicability. With the development of nanotechnology, metal nanoparticles (NPs), including Au, Ag, Pt, Pd and so on for sensing H_2O_2 have been received increased attention for its high stability, good biocompatibility and conductivity.[7] Among them, silver nanoparticles (Ag NPs) have drawn much attention, particularly in colorimetric detection due to their high extinction coefficients, high sensitivity, low-cost and simplicity.[8]

However, Ag NPs are very unstable in water and tend to oxidize and aggregate.[9] These disadvantages hinder their long-term storage, and ultimately limiting their application in H_2O_2 sensing. So how to overcome these problems becomes a vital issue. Generally, the aggregation of metal nanoparticles can be prevented either by electrostatic or steric stabilization. Therefore, surfactants such as sodium dodecyl sulphate (SDS),[10] cetyltrimethylammonium bromide (CTAB),[11] and some polymers including polyethylene glycol,[12] polyvinylpyrrolidone (PVP),[13] polyacrylonitrile (PAN),[14] poly(methyl methacrylate),[15] polyaniline[16] and poly (vinyl alcohol)[17] are widely used to stabilize Ag NPs. However, Pluronic F127, a nonionic triblock copolymers of poly(ethylene oxide)-block-poly(propylene oxide)-block-poly(ethylene oxide) with an average molecular weight of 12,600 and 70 wt. % PEO content,[18] has been barely used.[19]

Pluronics are made up of poly(ethylene oxide)-poly(propylene oxide)-poly(ethylene oxide) (PEO-PPO-PEO) in which PPO is the hydrophobic segment and contributes for 30 % of the block copolymer; whereas, PEO is a dominant hydrophilic segment of the block copolymer. Pluronics have been known to exhibit unique surface activity, micellization and reversible thermorheological phase behavior in water for many decades. They are highly surface active compounds and tend to form core-shell micelles with core consisting of hydrophobic middle PPO block surrounded by an outer shell of the hydrated hydrophilic PEO end blocks above the critical micelle concentration (cmc) or critical micelle temperature (cmt) in water.[20] Among various types of Pluronics, F127 has gained considerable attention due to its wide application on drug delivery[21] and porous structure formation.[22]

However, due to the nonionic nature, it is difficult to immobilize and stabilize Ag NPs using F127 alone, and the introduction of a sticking agent could be a good solution to this problem. As is well-known, dopamine (DA) has been reported to provide a facile approach to surface modification in which self-polymerization of dopamine produces an adherent poly(dopamine) (Pda) coating on noble metals, metal oxides, polymers and ceramics.[23] Therefore, the modification of F127 with Pda can introduce a versatile chemical coating, yielding F127 with strong adsorption for Ag NPs. Moreover, DA contains two hydroxyl groups at the ortho-positions to one another, ensuring it to have the abilities to reduce metal ions to metal nanoparticles, such as Au^{+} and Ag^{+}.[24] Thus, Ag NPs can be generated and subsequently stabilized via in situ reduction of the corresponding silver salts on the F127 micelles. By combining the remarkable reductive and adhesive property of DA and anisotropic self-assembly of F127, a novel Ag@DA@F127 system used for colorimetric detection of H_2O_2 could be fabricated.

Herein, a simple method using DA and F127 simultaneously to reduce and stabilize Ag NPs has been proposed (**Scheme 1**). The as-formed Ag@DA@F127 system was directly used for colorimetric detection of H_2O_2, without additional chromogenic agent. Moreover, with the aid of a simple UV-vis spectrophotometer, the

Ag@DA@F127 system can be used to detect H_2O_2 quantitatively. This system was proved to have a good performance in sensitivity, selectivity, linearity for the detection of H_2O_2. The linear range is from 0.1 μM to 100 μM, deriving a detection limit of 33 nM.

Experimental

Chemicals

F127 and dopamine hydrochloride were purchased from Sigma Aldrich. Silver nitrate ($AgNO_3$) was obtained from Jinzhujiang Chemical Co. Ltd (Guangzhou, China). Hydrogen peroxide solution (30 wt. %) was acquired from Aladdin Company (Shanghai, China). Sodium hydroxide (NaOH), sodium ascorbate, glucose (GLU), hydrochloride, uric acid (UA) and other chemical reagents were obtained from Sinopharm Chemical Reagent Co. Ltd. All reagents were at least of analytical grade and used as received. Deionized (DI) water (18.2 MΩ cm) was produced by ultrapure water systems (Ulupure Co. Ltd., Shanghai, China).

Preparation of Ag@DA@F127 system

Typically, 10 mg of F127 was added to 10 mL ultrapure water and dissolved with continuous magnetic stirring at 60 °C for 12 h, the resultant F127 solution was incubated at 60 °C for 24 h without agitation. Then 200 μL dopamine hydrochloride (4.42 mmol L^{-1}) and 100 μL sodium hydroxide (0.1 mol L^{-1}) were sequentially added to the F127 solution in order to form a reducing environment. After 20 min, $AgNO_3$ (8 mmol L^{-1}) was added dropwise to the above solution with stirring slowly. Immediately, the solution color turned from colorless to yellow, suggesting the formation of Ag@DA@F127 system.

Characterization

Transmission electron microscope (TEM) analysis was performed using a Tecnai TEM instrument (Tecnai G2 F20, FEI) with an accelerating voltage of 200 kV to characterize the high resolution transmission electron microscopy (HRTEM). Besides,

H-7650 (Hitachi) TEM was also employed to characterize the morphology of the samples. Specimens for TEM observations were prepared by drop-casting one drop of freshly prepared solutions on a copper grid coated with carbon, which was placed onto a filter paper to blot away the excess solution and drying slowly in air naturally.

The morphologies of the as prepared samples were characterized by atomic force microscope (AFM) in a tapping mode. ANTEGRA Prima system (NT-MDT, Zelenograd, Russia) and Si probes (NSG10, NT-MDT) were used. The samples were fabricated by spin-coating (2500 rpm, 60 s) the corresponding solutions at room temperature on the pre-cleaned silicon wafers.

Dynamic light scattering (DLS) was measured on the Malvern Zetasizer Nano ZS90 (Worcestershire, UK) at 25 °C with a He–Ne laser at 633 nm to obtain the hydrodynamic diameters and the zeta potentials of the sample solutions.

X-ray photoelectron spectrometer (XPS) measurements were taken via an ESCALAB250Xi (Thermo Scientific, USA) using a unmonchromatic Al *Kα* line at 1486.6 eV in an ultra-high-vacuum system with a base pressure 3×10^{-9} mbar and an analyzer pass energy of 150 eV, giving a full width at half-maximum of 1.7 eV for the Au $4f_{7/2}$ peak. The binding-energy scale was calibrated by assigning the main C1s peak at 284.8 eV. The XPS core-level spectra were analyzed by decomposing each spectrum into individual mixed Gaussian–Lorentzian peaks.

UV-vis spectra were recorded on a UV-2550 UV-vis spectrophotometer (Shimadzu Corp. Japan) with a 0.3 cm quartz cell and a bandwidth setting of 1 nm at a scan speed of 1200 nm min^{-1}.

Small-angle X-ray scattering (SAXS) experiments were carried out at 1W2A beam line of Beijing Synchrotron Radiation Facility (BSRF) with a Cu Kα wavelength of 1.54 Å. [25] SAXS patterns were collected with a 2D detector (MAR165 CCD; 2048×2048 pixels) placed at a distance of 5.01 m from the sample. The samples were fabricated by dip-coating the corresponding solutions at room temperature.

Colorimetric Assay of H_2O_2

The detection of H_2O_2 is conducted by the following procedure: 1 mL of the as-prepared Ag@DA@F127 solution and H_2O_2 solution within a range of 0~100 μM were added sequentially into a 1.5 mL tube. The reaction mixtures were then incubated at room temperature for more than 1 h, and the absorption spectra in the range of 300~600 nm are recorded. At the same time, the Ag@DA system for colorimetric assay of H_2O_2 is also taken in the similar way as a contrast. A_0 and A represent the absorbance at ~405nm of Ag@DA@F127 system in the absence and presence of H_2O_2.

Selectivity of Ag@DA@F127 system toward H_2O_2

The selectivity of the Ag@DA@F127 system was investigated using glucose, ascorbic acid, uric acid and several metal ions Cu^{2+}, Na^{+}, Ca^{2+}, Fe^{2+}, Mg^{2+}, K^{+}. They were individually added into 1 mL Ag@DA@F127 solutions and their final concentrations were adjusted to 50 μM. The reaction mixtures were then incubate at room temperature for more than 1h, and the absorption spectra in the range of 300~600 nm are recorded. The absorbance decrease in ~405 nm of Ag@DA@F127 system were also calculated, i.e. A_0-A.

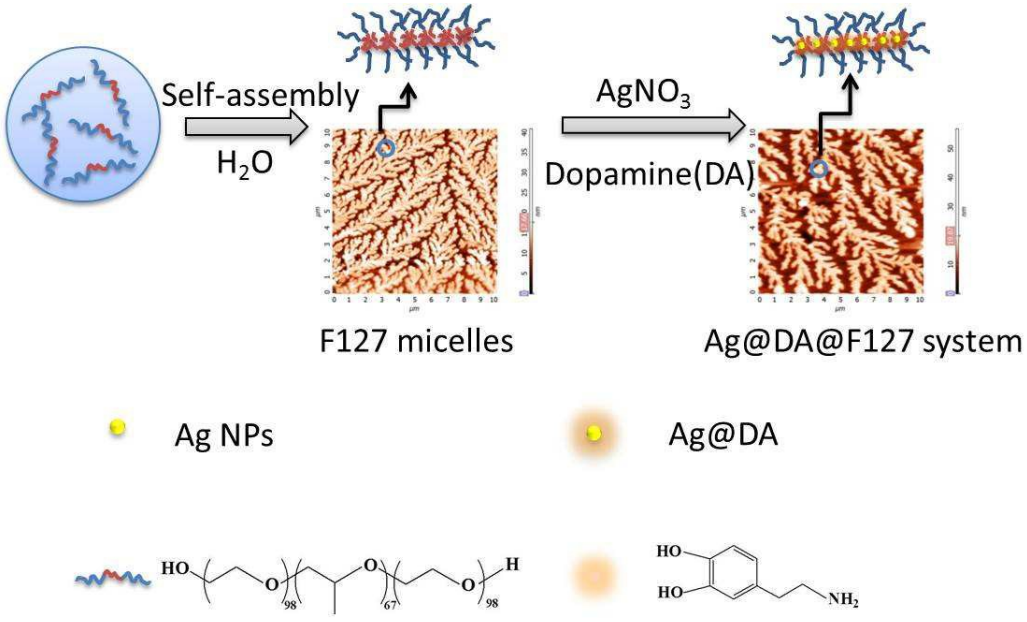

Scheme 1 Schematic illustration of the proposed mechanism of Ag@DA@F127 system formation and structure.

Results and Discussion

Characterization of Ag@DA@F127 system

The morphologies of the samples were characterized by transmission electron microscopy (TEM), and the typical TEM images of Ag@DA system, F127 micelles and Ag@DA@F127 system were respectively given in **Fig. 1**. The size of individual Ag NPs in Ag@DA system is between 5~20 nm and their shape is spherical, but they tend to form large clusters of approximately 200~300 nm in the presence of DA (**Fig. 1a**). The heavily aggregation behavior may be caused by the inherent aggregation characteristics of Ag NPs.[26] More importantly, slightly excessive DA may easily stick to each other due to its universal adhesive properties,[23] which in turn intensified the aggregation.

Fig. 1b shows that the F127 micelles can form network-like structure in the concentration of 0.1 wt.% without any other addictive (the critical micelle concentration (cmc) is 0.26–0.8 wt. %[27]). Generally, low concentration of copolymer remains molecularly dissolved in water and does not micellize. On heating the solution at 60 °C and further incubated for 24 h, the turbidity develops which resembles the clouding behavior of homo-poly(propylene oxide).[20] In the network-like F127 micelles, hydrophilic PEO block makes F127 dispersible in water, whereas the hydrophobic PPO block permits assembly with other hydrophobic building blocks. The above stable interactions led to the formation of a large scale network-like structure which is larger than 500 nm. Thus**,** this network-like structure will effectively prevent the aggregation of Ag NPs in Ag@DA@F127 system（**Fig. 1c**）. The narrow sized Ag NPs are anisotropically assembled in the network-like F127 micelles without any particle aggregation. Without using other reducing agents, Ag NPs in F127 micelles were synthesized with the help of exceptional adhesive and reductive self-polymerized polydopamine (Pda). As clearly indicated in the particle size distribution histogram (inset, **Fig.1c**), the main size of Ag NPs is ca. 5~10 nm and more homogeneous than that in Ag@DA system. Moreover, the particle size and

shape are not affected by F127, indicating that F127 does not interfere with the growth of individual Ag NPs.[28] The network-like F127 micelles perform like a skeleton to immobilize Ag NPs, which can well improve the dispersibility of nanoparticles. Meanwhile, the PEO blocks of F127 spread towards the aqueous solution, ensuring the stability of Ag@DA@F127 system which could be also manifested from the nearly constant data of zeta potential (ζ), ca. -33 mV, while the Ag@DA system and F127 micelles are as the contrast (**Fig. S1**†). Moreover, the corresponding Ag@DA@F127 solutions can remain stable and no sediment can be found over 24 h (**Fig. S2**†).

Besides, high resolution transmission electron microscopy (HRTEM) imaging (**Fig. 1d**) shows that the spacing between two adjacent lattice planes is about 0.24 nm, which is in agreement with the spacing of the (111) plane of the Ag crystal.[29]

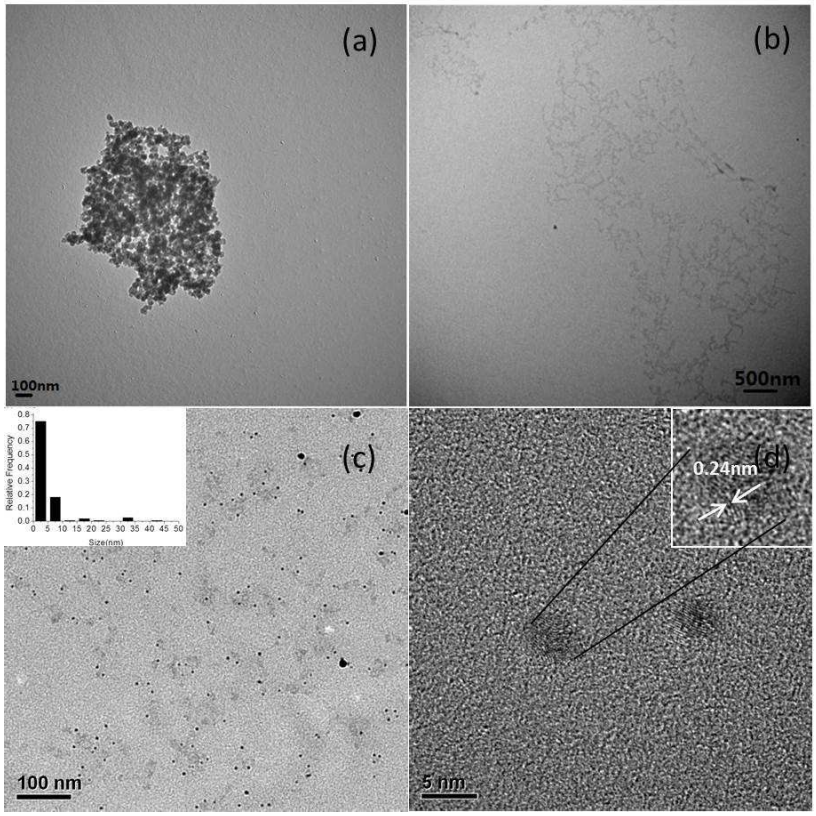

Fig. 1 TEM images of (a) Ag@DA system (65/35 wt. %); (b) F127 micelles (0.1 wt. %, 1 mg mL^{-1}); (c) Ag@DA@F127 system (2.6/1.4/96 wt. %), the inset shows the particle size distribution

histogram; (d) The HTEM images of Ag NPs immobilized in Ag@DA@F127 system (2.6/1.4/96 wt. %), the inset shows the magnified Ag NPs.

DLS data reveals the hydrodynamic diameters of the corresponding samples in aqueous solution, the Ag@DA system, F127 micelles and Ag@DA@F127 system are ~22 nm, ~119 nm and ~51 nm, respectively (**Fig**. **2**). The variation trend of DLS diameters is in agreement with the TEM results (**Fig**. **1**). It is obvious that the hydrodynamic diameter in F127 micelles is larger than the others', which is owing to its large scale network-like structure as seen in TEM image in **Fig. 1b**. Therefore, the Ag@DA@F127 system with Ag NPs anisotropic self-assembled in the network-like F127 micelles possesses an increased hydrodynamic diameter compared to the Ag@DA system, which can also prove the immobilization of Ag NPs in the network-like F127 micelles.

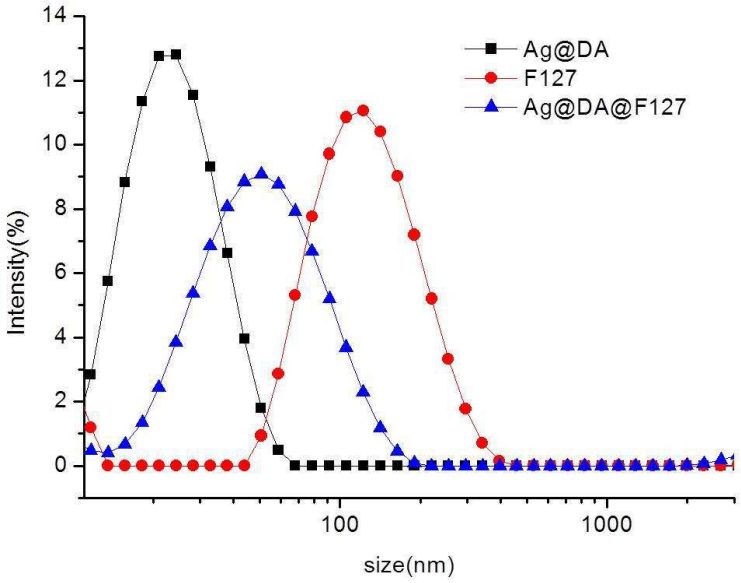

Fig. 2 DLS size distribution of Ag@DA system, F127 micelles and Ag@DA@F127 system.

AFM images in **Fig. 3** are further collected to confirm the structures indicated in TEM results. Well-dispersed spherical particles with size of ca. 100~200 nm can be clearly seen, and it can be inferred that the particles are the clusters of Ag NPs instead of individual nanoparticles (**Fig. 3a)**. Notably, dendritic structures corresponding to

F127 micelles and Ag@DA@F127 system can be found in **Fig. 3b** and **Fig. 3c**, respectively. The dendritic structures are in accordance with the network-like structures observed via TEM and could be attributed to the crystallization of PEO units of F127, which was reported in the thin film flat-on lamellae of PEO blocks.[30, 31] Although F127 micelles and Ag@DA@F127 system both have the similar dendritic structure, the average diameter and height of the branches of dendritic structures in Ag@DA@F127 system is ~1μm and ~23 nm, respectively, which are larger than ~0.5 μm and ~17 nm of F127 micelles. We speculate that these may result from the immobilization of Ag NPs in F127 micelles and the adhesion of adjacent micelles caused by the sticking agent, i.e. dopamine. The above AFM results show that the Ag@DA system cannot form a long-range order structure, while the Ag@DA@F127 system forms a network-like structure. This is proven by using the SAXS setup.[25] Compared with the Ag@DA system (**Fig. S3a**†), Ag@DA@F127 system has a diffraction ring (**Fig. S3b**†), indicating the existence of Ag NPs. The pattern of Ag@DA@F127 system is oriented in the horizontal direction, owing to the anisotropy self-assemble of Ag NPs (**Fig. S3c**†).

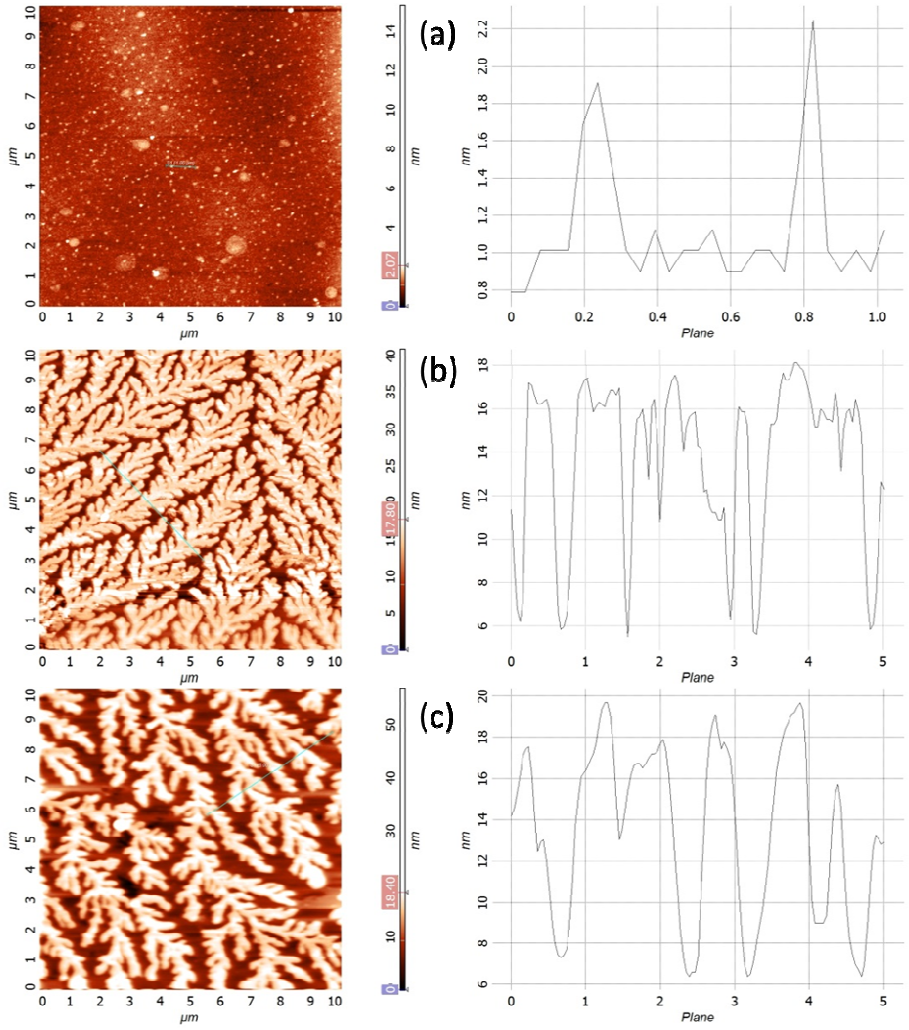

Fig. 3 (Left) AFM images of (a) Ag@DA system (65/35 wt. %), (b) F127 micelles (0.1 wt. %, 1mg mL^{-1}) and (c) Ag@DA@F127 system (2.6/1.4/96 wt. %). (Right) cross-section profiles of the marked positions corresponding to the height images.

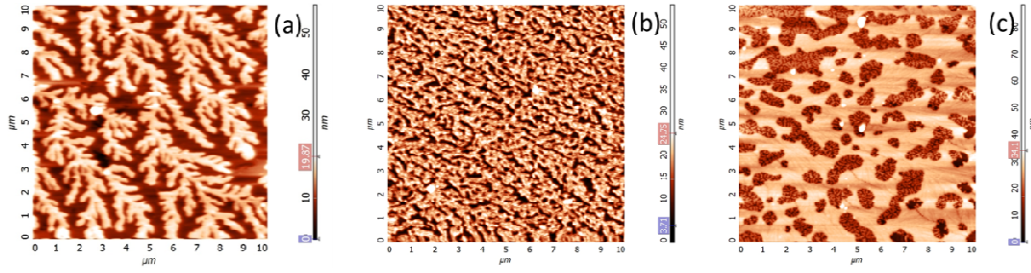

Fig. 4 AFM images of Ag@DA@F127 system with different concentrations of F127, (a) 1 mg mL^{-1}, (b) 1.5 mg mL^{-1} and (c) 2 mg mL^{-1}.

It's noteworthy that the concentration of F127 will dramatically affect the structure of Ag@DA@F127 system. As indicated in the series of AFM images of

Ag@DA@F127 system with different F127 concentrations in **Fig. 4**, the network-like structures disappear in high concentrations, which is unfavorable for the dispersibility of Ag NPs.

To better understand the mechanism underlying the formation of the Ag@DA@F127 system, the results obtained are further rationalized by X-ray photoelectron spectroscopy (XPS) analysis regarding the element components and the chemical state of the elements in the as-prepared samples. As shown in the XPS survey spectra, distinct O1s peak and C1s peaks can be found both in Ag@DA system and Ag@DA@F127 system (**Fig. 5a**). In Ag@DA@F127 system (2.6/1.4/96 wt. %), Ag3d peak and N1s peak are hard to find owing to the small proportion of Ag NPs and DA while in Ag@DA system (65/35 wt. %), the Ag3d peak and N1s peak are obvious. As referred in the above TEM analysis, F127 micelles in Ag@DA@F127 system do not interfere with the growth of individual Ag NPs. So the chemical state of Ag NPs in Ag@DA system is similar to Ag@DA@F127 system and can be used for the Ag analysis to some extent. As can be seen in **Fig. 5b**, Ag NPs exhibits two specific peaks with binding energies of 368.0 eV and 374.0 eV, which are attributed to $Ag3d_{5/2}$ and $Ag3d_{3/2}$ electrons of Ag^0, respectively. The spin energy separation was identified as 6.0 eV, which indicates the formation of Ag NPs.[32] Moreover, the XPS spectra of Ag $3d_{5/2}$ show that there are two components after deconvolution, attributed to Ag^+ (368.2eV) and Ag^0 (367.7eV), respectively.[32] It can conclude that the silver mainly existed in Ag^0, $AgNO_3$ as the original reactant was partly reduced into Ag^0. The main types of C1s peaks at 284.5 eV, 285.7 eV, 286.5 eV, and 288.7 eV are assigned to C-C, C-N, C-O, and C=O, respectively (**Fig. 5c** and **5d)**. More specifically, C1s XPS spectra corresponding to pure DA and Ag@DA system show the intensity change of DA in the addition of $AgNO_3$. The peak for the C-O species shown in pure DA almost disappears in Ag@DA system, implying more oxygen-containing functional groups reacted or were removed. Furthermore, the appearance of C=O peak in Ag@DA system reveals the appearance of quinone structure which was formed by the two hydroxyl groups at the ortho positions in the molecule of DA.[8] Moreover, the

quinone groups would adsorb on the surface of Ag NPs and the alkylamines were left outside to stabilize Ag NPs. Notably, the decrease of R-NH_2 peak and the increase of =N-R peak in the N1s XPS spectra indicate the polymerization of DA, which produces an adherent Pda coating on F127 micelles (**Fig. S4a†** and **Fig. S4b†**). Therefore, the versatile chemical coating of Pda yields F127 with strong adsorption for Ag NPs, functioning as a sticking agent to assist F127 micelles to immobilize and stabilize Ag NPs. Similar to DA, F127 can also function as a reducing agent, owing to its plenty of hydroxyl groups in the PEO blocks,[33] and this aspect is demonstrated in the O1s XPS spectra of F127 micelles and Ag@DA@F127 system (**Fig. 5e** and **5f)**. A distinct decrease of O-H peak intensity can be clearly found, inferring that the hydroxyl groups in the F127 micelles have been reacted. Moreover, the C1s XPS spectra of F127 micelles and Ag@DA@F127 system can also support this point (**Fig. S4c†** and **Fig. S4d†)**, and a comparatively small decrease on the intensity of the C-O peak is observed. The reaction mechanism might be as follows:

$$R\text{-}OH + Ag^{+} \rightarrow R\text{-}O\text{-}Ag + H^{+}$$

$$R\text{-}O\text{-}Ag + Ag^{+} \rightarrow R{=}O + Ag^{0}$$

$$R\text{-}OH + Ag^{+} \rightarrow R{=}O + Ag^{0} + H^{+}$$

Here, R-OH represents the hydroxyl groups in both DA and F127, R=O represents the oxidation of hydroxyl groups while H^{+} is an acid byproduct HNO_3.[34]

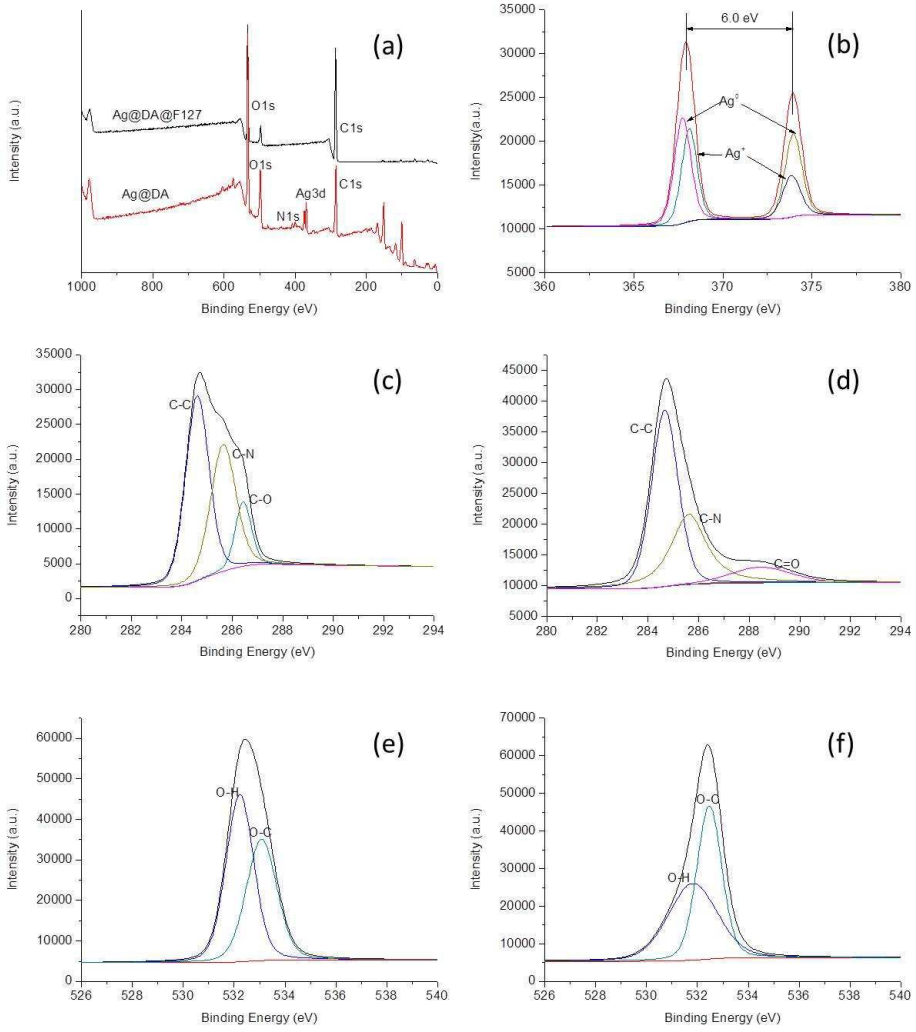

Fig. 5 (a) XPS survey spectra of Ag@DA@F127 system (2.6/1.4/96 wt. %) and Ag@DA system (65/35 wt. %); (b) Ag 3d XPS spectrum of Ag@DA system; C1s XPS spectra of (c) pure DA; (d) Ag@DA system (65/35 wt. %); O1s XPS spectra of (e) F127 micelles and (f) Ag@DA@F127 system (2.6/1.4/96 wt. %).

The above XPS analysis results have shown that there are abundant hydroxyl and amino groups on DA and F127. These groups ensure the excellent stability and hydrophilicity of Ag@DA@F127 system as well reflected in the ζ analysis (**Fig. S1**†). The surface of Ag@DA system, pure F127 micelles and Ag@DA@F127 system are all negatively charged. In particular, the ζ of Ag@DA@F127 system stay around a stable value at approximately -33 mV compared to the Ag@DA system, which ensure the Ag@DA@F127 solution keep stable for months.

The optical properties of the samples are further investigated. **T**he Ag@DA@F127 system display absorption peaks at ~405 nm, which is attributed to the surface plasmon resonance of the Ag NPs (**Fig. 6**).[35] In contrast, the UV-vis absorption spectra of fresh Ag@$NaHB_4$@F127, Ag@DA and Ag@DA@F127 aqueous solutions are shown respectively (**Fig. S5†**). The full width at half maximum of absorption peak in Ag@DA@F127 system is slight larger than that of Ag@DA system, because the formation of anisotropic self-assembled Ag NPs in Ag@DA@F127 system leads to a larger scattering component of the spectrum. The absorbance peak of fresh Ag@$NaHB_4$@F127 system is weaker than the others, and an obvious shoulder peak can be found at 500~600 nm which indicates that the Ag NPs reduced by $NaHB_4$ tend to heavily aggregate without DA. As referred in the experimental section, with $AgNO_3$ added dropwise to the F127 solution, the mixture color turned from colorless to yellow, indicating the formation of Ag@DA@F127 system. However, the color of Ag@$NaHB_4$@F127 aqueous solution changes from dark red to black with the increase of standing time (**Fig. S2†**). That is to say, the Ag NPs in Ag@$NaHB_4$@F127 system will quickly aggregate and oxidize after the preparation. Conversely, DA can play a dual role in the Ag@DA@F127 system, functioning as both reducing agent and sticking agent in Ag@DA@F127 system and thus ensure the system's outstanding stability.

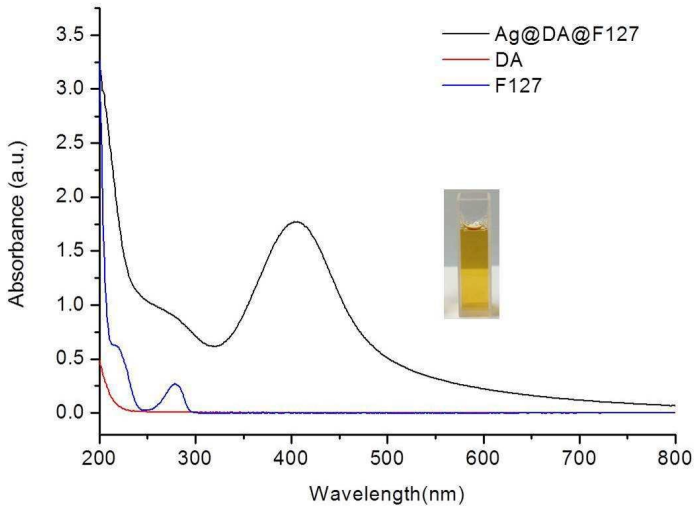

Fig. 6 UV-vis absorption spectra of Ag@DA@F127, F127 and DA aqueous solutions; Inset: photographs of Ag@DA@F127 aqueous solutions.

Colorimetric Detection of H_2O_2

The sensitivity of Ag@DA@F127 system to H_2O_2 is further investigated. The higher H_2O_2 concentration, the stronger decrease in the Ag NPs concentration and hence, lowering surface plasmon resonance peak intensity (**Fig. 7**). At the same time, the yellow color fades in varying degree depending on the H_2O_2 concentration (inset in **Fig. 7**). It can be concluded that oxidation of Ag NPs by H_2O_2 leads to the degradation and decolorization of nanoparticles ($Ag + 2H_2O_2 \rightarrow Ag^+ + O_2^{\bullet -} + 2H_2O$).[36]

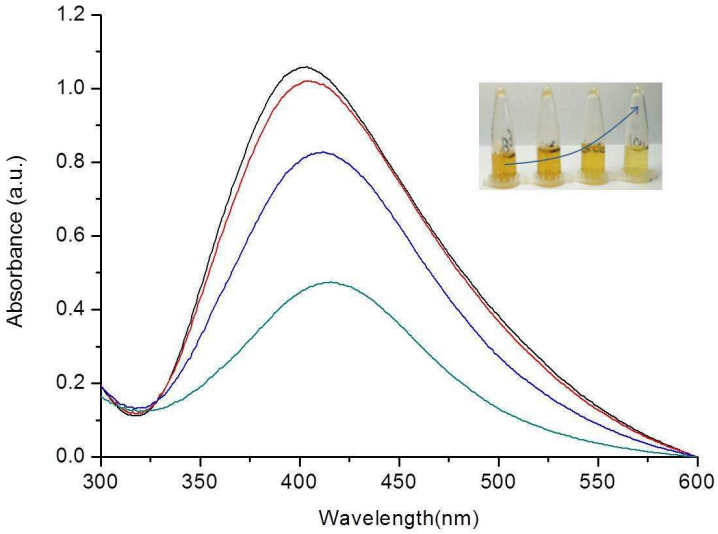

Fig. 7 UV−vis absorption spectra of Ag@DA@F127 aqueous solutions and Ag@DA@F127 aqueous solutions in the presence of 10, 100, 1000 μM H_2O_2. Inset: the corresponding photographs of Ag@DA@F127 aqueous solution in the presence of 0, 10, 100, and 1000 μM H_2O_2.

The above observation provides Ag@DA@F127 system a potential for quantitative detection of H_2O_2. **Fig. 8a** shows the UV-vis absorption spectra of the Ag@DA@F127 system in the presence of various amounts of H_2O_2, and the variation in absorbance at ~405 nm shows a wide range linearity from 0.1 μM to 100 μM H_2O_2

concentration with linear regression coefficient (r^2) of 0.99056 (**Fig. 8b**). The limit of detection (LOD) is calculated by a signal-to-noise ratio of 3 (3σ/S). Here, S means the slope of the linear equation and σ means the standard deviation of blank measurements. Thus, the detection limit DL = 3(0.0786/0.00715) =33 nM.[37] As a contrast, Ag@DA system shows linearity from 10 μM to 60 μM, which is narrower than Ag@DA@F127 system **(Fig. S6†)**. **Table 1** summarizes some recent reports on the H_2O_2 sensing based on utilizing Ag NPs, Ag NPrs (silver nanoprisms) or Ag NCs (silver nanocrystals) combined with either colorimetric, electrochemistry or fluorimetry approach.[38-44] Compared with reported detection for H_2O_2, our system exhibits a superior performance especially a low detection limit. The good performance of Ag@DA@F127 system benefited from the larger surface area of Ag NPs whose dispersibility was improved by the network-like F127 micelles. Moreover, compared to the traditional methods, this system shows its easy processibility and environmentally friendly feature.

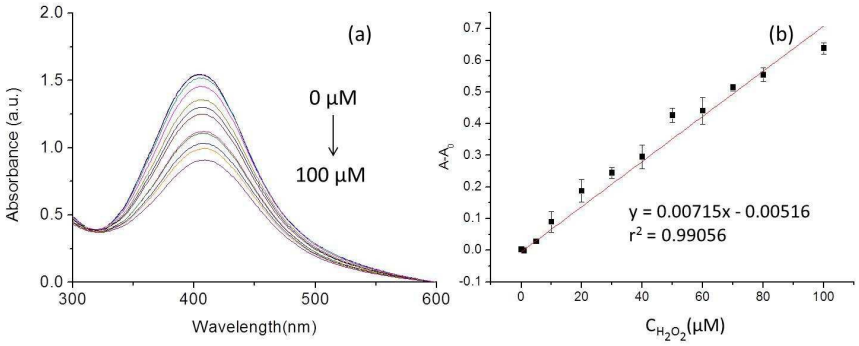

Fig. 8 (a) UV−vis absorption spectra of Ag@DA@F127 system in the presence of 0, 0.1, 1.0, 5, 10, 20, 30, 40, 50, 60, 70, 80, and 100 μM H_2O_2; (b) plot of absorbance decrease versus H_2O_2 concentration (0.1~100 μM).

Table 1 Comparison of other silver-based sensors for the determination of hydrogen peroxide (H_2O_2)

NO.	Material	Detection approach	Linear range	Limit of detection	Ref.
1	Ag NPs[a]	Electrochemistry	100μM-260mM	4μM	37
2	Ag NPs	Electrochemistry	100μM-10mM	7μM	38
3	Ag NCs[b]	Fluorimetry	0.5μM-100μM	0.4μM	39
4	Ag NS	Spectrophotometry	1μM -100mM	0.9 μM	40
5	Ag NS	Spectrophotometry	1μM -100mM	1 μM	41
6	Ag NS	colorimetric	0.3μM -3μM	0.3 μM	42
7	Ag NPrs[c]	colorimetric	10μM -80μM	6.19 μM	43
8	Ag NS	colorimetric	0.1μM -100μM	33 nM	This work

[a] Ag NPs = silver nanoparticles; [b] Ag NCs = silver nanocrystals; [c] Ag NPrs = silver nanoprisms.

Finally, the selectivity of the Ag@DA@F127 system toward H_2O_2 was evaluated. For this aim, 50 μM H_2O_2, glucose, ascorbic acid, uric acid, Cu^{2+}, Na^{+}, Ca^{2+}, Fe^{2+}, Mg^{2+}, and K^{+} were added individually into the Ag@DA@F127 system. **Fig. 9** shows the absorbance decrease in ~405 nm of Ag@DA@F127 system toward H_2O_2, glucose, ascorbic acid, uric acid, Cu^{2+}, Na^{+}, Ca^{2+}, Fe^{2+}, Mg^{2+}, and K^{+}. As indicated, the Ag@DA@F127-based detection system exhibits a highly selective response to H_2O_2. Besides, the negative signal of ascorbic acid is owing to its reducibility. In the Ag@DA@F127 solution, a slight oxidation reaction of Ag NPs may occurred and the addition of ascorbic acid may suppress it.

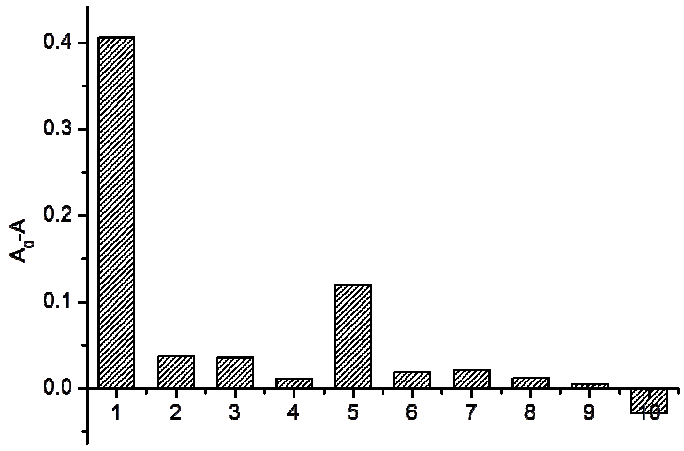

Fig. 9 Absorbance decrease of the Ag@DA@F127 system in the presence of 50 μM of (1) H_2O_2; (2) Fe^{2+}; (3) Na^+; (4) K^+; (5) Cu^{2+}; (6) Mg^{2+}; (7) Ca^{2+}; (8) Glucose; (9) Uric acid and (10) Ascorbic acid.

Conclusions

In summary, we have synthesized well-dispersed and anisotropically self-assembled Ag NPs in the network-like F127 micelles by a facile and green method. The use of dopamine can reduce silver nitrate to Ag NPs and subsequently stick them to the F127 micelles. Thus, a ternary system, i.e. Ag@DA@F127 was constructed. The fabricated Ag@DA@F127 system exhibited a high sensitive and quantitative detection of H_2O_2 over a wide linear range from 0.1 μM to 100 μM and a low detection limit of 33 nM. The linear regression coefficient (r^2) is calculated to be 0.99056. Compared to the control system of Ag@DA, the Ag@DA@F127 system shows a wider detection range and a lower detection limit owing to the good dispersion and stability of Ag NPs in the presence of network-like F127 micelles. Furthermore, this making method is simple and environmentally friendly. Therefore, the combination of these unique characteristic properties of the Ag@DA@F127 system makes it preferable in H_2O_2 detection.

Acknowledgements

SAXS data were obtained at 1W2A, Beijing Synchrotron Radiation Facility (BSRF). The authors gratefully acknowledge the assistance of scientists from BSRF during the experiments. This work was supported by the National Natural Science Foundation of China (21072221, 21172252).

Notes and references

1. W. Lei, A. Durkop, Z. H. Lin, M. Wu and O. S. Wolfbeis, *Microchimica Acta*, 2003, **143**, 269-274.
2. J. Wang, Y. H. Lin and L. Chen, *Analyst*, 1993, **118**, 277-280.
3. S. Hanaoka, J. M. Lin and M. Yamada, *Analytica Chimica Acta*, 2001, **426**, 57-64.
4. M. Hoshino, S. Kamino, M. Doi, S. Takada, S. Mitani, R. Yanagihara, M. Asano, T. Yamaguchi and Y. Fujita, *Spectrochimica Acta Part a-Molecular and Biomolecular Spectroscopy*, 2014, **117**, 814-816.
5. I. Mori, K. Takasaki, Y. Fujita and T. Matsuo, *Talanta*, 1998, **47**, 631-637.
6. W. J, *Chemical Reviews*, 2008, **108**.
7. S. Chen, R. Yuan, Y. Chai and F. Hu, *Microchimica Acta*, 2013, **180**, 15-32.
8. Y. Ma, H. Niu, X. Zhang and Y. Cai, *Analyst*, 2011, **136**, 4192-4196.
9. Z. Zhang, J. Zhang, B. Zhang and J. Tang, *Nanoscale*, 2013, **5**, 118-123.
10. T. Sinha, V. Gude, N. V. S. Rao, T. Sinha and V. Gude, *Advanced Science*, 2012, **volume 4**, 381-387(387).
11. G. Wei, L. Wang, H. Zhou, Z. Liu, Y. Song and Z. Li, *Applied Surface Science*, 2005, **252**, 1189-1196.
12. C. C. Luo, Y. H. Zhang, X. W. Zeng, Y. W. Zeng and Y. G. Wang, *Journal of Colloid and Interface Science*, 2005, **288**, 444-448.
13. M. P. Zheng, M. Y. Gu, Y. P. Jin and G. L. Jin, *Materials Research Bulletin*, 2001, **36**, 853-859.
14. Z. P. Zhang, L. D. Zhang, S. X. Wang, W. Chen and Y. Lei, *Polymer*, 2001, **42**, 8315-8318.
15. N. Singh and P. K. Khanna, *Materials Chemistry and Physics*, 2007, **104**, 367-372.
16. P. K. Khanna, N. Singh, S. Charan and A. K. Viswanath, *Materials Chemistry and Physics*, 2005, **92**, 214-219.
17. Y. Zhou, S. H. Yu, C. Y. Wang, X. G. Li, Y. R. Zhu and Z. Y. Chen, *Advanced Materials*, 1999, **11**, 850-+.
18. M. Fukao, A. Sugawara, A. Shimojima, W. Fan, M. A. Arunagirinathan, M. Tsapatsis and T. Okubo, *Journal of the American Chemical Society*, 2009, **131**, 16344-16345.
19. D. G. Angelescu, M. Vasilescu, M. Anastasescu, R. Baratoiu, D. Donescu and V. S. Teodorescu, *Colloids and Surfaces a-Physicochemical and Engineering Aspects*, 2012, **394**, 57-66.
20. K. Nakashima and P. Bahadur, *Advances in Colloid and Interface Science*, 2006, **123**, 75-96.
21. Z. Wei, J. Hao, S. Yuan, Y. Li, W. Juan, X. Sha and X. Fang, *International Journal of Pharmaceutics*, 2009, **376**, 176-185.
22. S. P. Naik, S. Yamakita, M. Ogura and T. Okubo, *Microporous & Mesoporous Materials*, 2004, **75**, 51–59.
23. H. Lee, S. M. Dellatore, W. M. Miller and P. B. Messersmith, *Science*, 2007, **318**, 426-430.
24. K. Yoosaf, B. I. Ipe, C. H. Suresh and K. G. Thomas, *Journal of Physical Chemistry C*, 2007, **111**, 12839-12847.
25. Z. Li, Z. Wu, G. Mo, X. Xing and P. Liu, *Instrumentation Science & Technology*, 2014, **42**, 128-141.
26. V. K. Sharma, K. M. Siskova, R. Zboril and J. L. Gardea-Torresdey, *Advances in Colloid & Interface Science*, 2014, **204**, 15–34.
27. Q. Gao, Q. Liang, Y. Fei, X. Jian, Q. Zhao and B. Sun, *Colloids Surf B Biointerfaces*, 2011, **88**, 741–748.

28. D. G. Angelescu, M. Vasilescu, R. Somoghi, D. Dan and V. S. Teodorescu, *Colloids & Surfaces A Physicochemical & Engineering Aspects*, 2010, **366**, 155-162.
29. X.-Z. Tang, Z. Cao, H.-B. Zhang, J. Liu and Z.-Z. Yu, *Chemical Communications*, 2011, **47**, 3084-3086.
30. C. M. Chan and L. Li, *Advances in Polymer Science*, 2005, **188**, 1-41.
31. S. L. Kotova, V. A. Timofeeva, G. V. Belkova, N. A. Aksenova and A. B. Solovieva, *Micron*, 2012, **43**, 445-449.
32. Q. Chen, W. Shi, Y. Xu, D. Wu and Y. Sun, *Materials Chemistry and Physics*, 2011, **125**, 825-832.
33. L. Y. Wang, X. Chen, J. K. Zhao, Z. M. Sui, W. C. Zhuang, L. M. Xu and C. J. Yang, *Colloids and Surfaces a-Physicochemical and Engineering Aspects*, 2005, **257-58**, 231-235.
34. E. Filippo, A. Serra and D. Manno, *Sensors and Actuators B-Chemical*, 2009, **138**, 625-630.
35. W. Wu, T. Zhou and S. Zhou, *Chemistry of Materials*, 2009, **21**, 2851-2861.
36. T. Wen, F. Qu, N. B. Li and H. Q. Luo, *Analytica Chimica Acta*, 2012, **749**, 56–62.
37. L. Chen, X. Fu, W. Lu and L. Chen, *Acs Applied Materials & Interfaces*, 2013, **5**, 284-290.
38. W. Lu, Y. Luo, G. Chang and X. Sun, *Biosensors & Bioelectronics*, 2011, **26**, 4791-4797.
39. Y. Zhang, S. Liu, L. Wang, X. Qin, J. Tian, W. Lu, G. Chang and X. Sun, *Rsc Advances*, 2012, **2**, 538-545.
40. T. Wen, F. Qu, N. B. Li and H. Q. Luo, *Analytica Chimica Acta*, 2012, **749**, 56-62.
41. P. Vasileva, B. Donkova, I. Karadjova and C. Dushkin, *Colloids and Surfaces a-Physicochemical and Engineering Aspects*, 2011, **382**, 203-210.
42. S. Mohan, O. S. Oluwafemi, S. C. George, V. P. Jayachandran, F. B. Lewu, S. P. Songca, N. Kalarikkal and S. Thomas, *Carbohydrate Polymers*, 2014, **106**, 469-474.
43. D.-M. Han, Q. M. Zhang and M. J. Serpe, *Nanoscale*, 2015, **7**, 2784-2789.
44. K. Nitinaivinij, T. Parnklang, C. Thammacharoen, S. Ekgasit and K. Wongravee, *Analytical Methods*, 2014, **6**, 9816-9824.

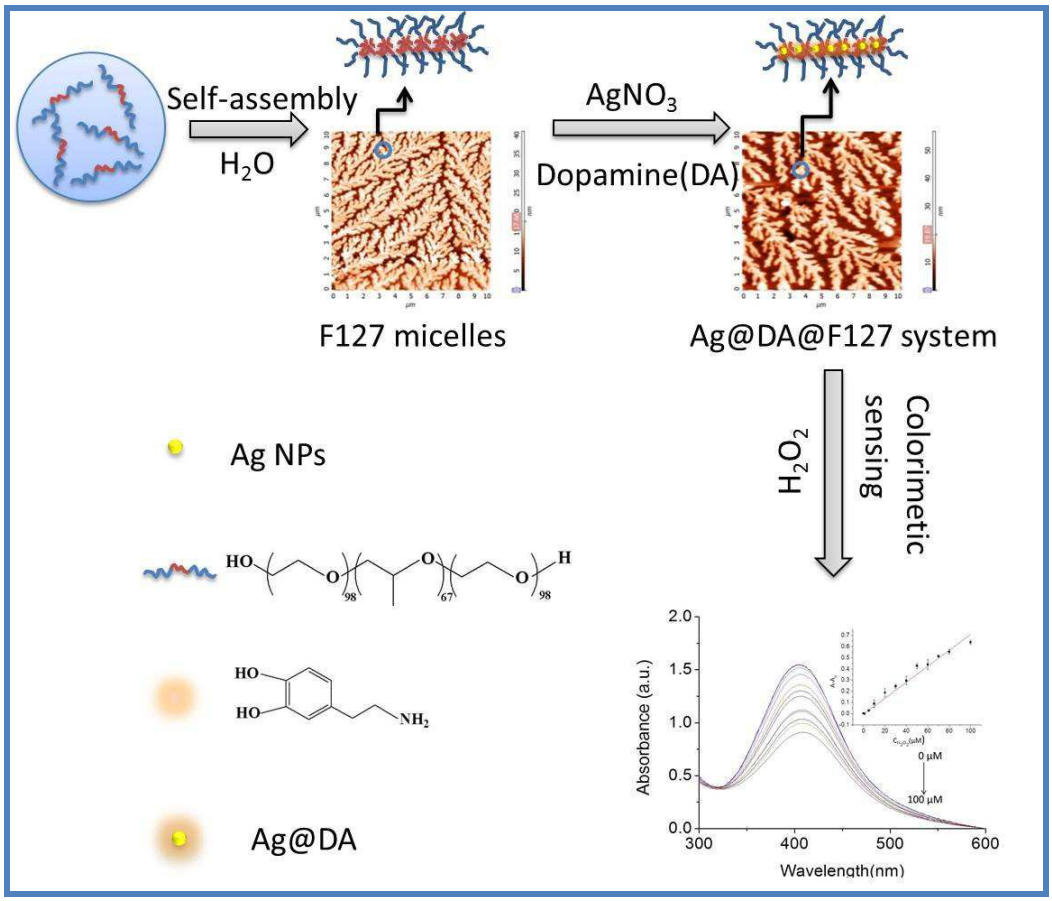

Table of Contents

Facile and green synthesis of Ag@DA@F127 system for the sensitive and quantitative detection of H_2O_2 over a wide linear range from 0.1 μM to 100 μM and a low detection limit of 33 nM. Ag NPs in the network-like F127 micelles were well-dispersed and anisotropically self-assembled, ensuring a large surface area, which makes it preferable in H_2O_2 detection.